PII: S0032-3861(96)00767-7

Polymer Vol. 38 No. 9, pp. 2077–2091, 1997

0032-3861/97/$17.00 + 0.00

Rheo-photoacoustic *FT* i.r. studies of thermal history–strain dependence in poly(vinylidene fluoride)

Bret W. Ludwig and Marek W. Urban*
Department of Polymers and Coatings, North Dakota State University, Fargo, ND 58105, USA
(Received 29 August 1995; revised 6 April 1996)

This study focuses on the effect of thermal history on the morphology of poly(vinylidene fluoride). Rheo-photoacoustic Fourier transform infra-red spectroscopy (RPA *FT*i.r.) was utilized to measure changes in PVDF network permeability as a function of elongation. The permeability data, in conjunction with the stress–strain response, provide insights into the morphological changes resulting from deformations. The rate at which the PVDF network is cooled from the melt, as well as morphological changes resulting from annealing, appear to have a substantially greater influence on the response of the network to deformations than molecular weight effects. Prior to deformations, the crystalline phase and the size of the individual crystals, appear to have the most effect on PVDF permeability. Following the application of stresses, the number of tie molecules have a dominating effect on the network permeability. Annealing PVDF within 20°C of its melting point (170°C) increases the yield stress and the Young's modulus values. Similar effects are detected upon reducing the cooling rate. © 1997 Elsevier Science Ltd.

(Keywords: rheo-photoacoustic *FT*i.r. spectroscopy; PVDF; thermal history)

INTRODUCTION

The fact that the permeability of semicrystalline polymers depends on the relative amounts of amorphous and crystalline phases is well documented[1–3]. The nature of the crystalline and amorphous phases is, in turn, affected by the molecular weight and thermal history of a polymer. While molecular weight is determined by the synthetic efforts involved in building macromolecules, the thermal history will be determined by cooling/heating rates as well as other factors. Thus, the crystalline/amorphous content can be controlled not only by the makeup of the macromolecular segments, but also by how much and at what rate kinetic energy is supplied or removed from a polymer network.

The amount of crystals nucleated in a molten polymer depends upon the degree of super cooling[4]. For example, a polymer which has a melting temperature of 170°C, and crystallizes at 150°C, is said to be supercooled by 20°C. Greater degrees of supercooling result in a larger number of crystals being nucleated in the network. Therefore, slower cooling allows spherulites nucleated in the first stages of cooling to expand further, prior to encountering other crystallization zones. This reduces the number of inter-spherulitic amorphous regions, and increases the degree of order in the network. The morphology of semicrystalline polymers which results from two extreme cases of crystallization is shown in *Figure 1*. For the sake of clarity, only tie molecules are shown in the amorphous phase. *Figure 1A* illustrates the large crystallites and spherulites which are produced by slowly cooling a network from the melt. *Figure 1B* shows the larger number of spherulites and small crystals produced by quenching a polymer network.

Since the rate of cooling determines the number and size of crystallites, it also affects the nature of the amorphous phase, which is reflected by the number of tie molecules and chain entanglements connecting neighbouring crystallites. Slower cooling rates reduce the kinetics of crystallization[4], which gives a polymer chain more opportunity to disentangle during crystallization. This process increases the perfection of the chain folded lamellae, and reduces the number of tie molecules and the chain entanglements.

Thermal treatments of polymer networks, such as annealing, quenching, supercooling, and other treatments, alter the morphology of semicrystalline polymers. Of particular importance is annealing which, for a semicrystalline polymer near its melting temperature, will result in melting of imperfectly formed crystals. Upon cooling, larger, more stable crystals will be formed[5].

The length of polymer chains, and therefore their molecular weight, will influence polymer network morphology. The influence of molecular weight on the crystalline phase results from the crystallization kinetics of linear segments. For example, increased molecular weight was demonstrated to result in more rapid crystal growth in poly(ethylene)[6], leading to the formation of larger crystals. Connecting the crystallites are amorphous tie molecules, which have segments embedded in the

* To whom correspondence should be addressed

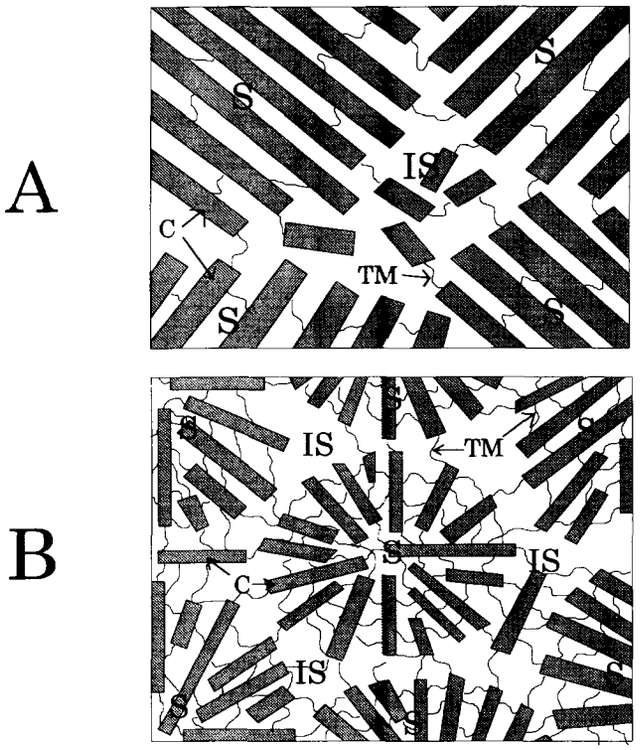

Figure 1 Schematic diagram of spherulitic morphology for: (A) semicrystalline polymers cooled slowly from the melt; (B) semicrystalline polymers quenched from the melt. S, spherulite; IS, interspherulitic region; C, crystal; TM, tie molecule

neighbouring crystals. When drawn taut by the application of stresses to the film, the tie molecules hinder the mobility of the amorphous phase chains, which reduces free volume and permeability. Since the number of tie molecules is linearly related to molecular weight of a polymer[7], molecular weight is expected to play a significant role in the permeability of polymer networks under external stresses.

With this background in mind, and considering our previous studies on PVDF, in which we have examined the effect of crystallinity on permeability[8], and diffusivity dependence on molecular weight[9], we expand the scope of these efforts and examine the influence of thermal history on permeability. Since elongation of PVDF also results in morphological changes, this study also examines the effect of external forces on permeability to PVDF. To identify interrelations between polymer molecular weight, morphology, thermal history, and network permeability, the permeability of 45 000 and 150 000 PVDF specimens will be determined under various conditions.

EXPERIMENTAL

Specimen preparation and spectral measurements

PVDF samples were obtained from Elf Atochem Inc. Ethyl acetate was acquired from Aldrich Chemical Co., and was used without further purification. 45 000 and 150 000 MW PVDF specimens were melt crystallized into $350 \pm 20\,\mu m$ thick films. Procedures describing the sample preparation were described in the previous paper[9]. Specimens were cooled from the melt (220°C) at rates of 20 or 3°C min^{-1}, or were quenched in an ice water bath. Selected specimens, cooled at a rate of 20°C min^{-1}, were subjected to annealing at 150 or 170°C for 18 h. In the case of fibrous samples, thermal treatments were conducted before the transformation from a spherulitic morphology. Dumbbell shaped samples with a length of 75 mm, end width of 14 mm, notch length of 25 mm, and notch width of 7 mm were cut from prepared films. Fibrous specimens were obtained by drawing dumbbell shaped samples at 25°C. All specimens were saturated by immersion in ethyl acetate (EtAc) for a minimum of 72 h prior to the determination of their transport properties.

Rheo-photoacoustic Fourier transform infra-red (RPA *FT*i.r.) spectroscopy was utilized to measure the rate of EtAc diffusion from PVDF specimens, as described elsewhere[8,9]. Quantitative determination of the desorption diffusion coefficient (D_d), from the spectroscopically acquired data was made possible by the use of a calibration curve presented in the preceding paper[9].

Differential scanning calorimetry and stress–strain measurements

D.s.c. and stress–strain measurements were performed according to procedures described elsewhere[9].

RESULTS AND DISCUSSION

Prior to examining the effect of thermal history on PVDF permeability, let us determine if the stress–strain response may provide insights about PVDF morphology. *Table 1* lists the yield stress (σ_y) and the Young's modulus (E) values, obtained from specimens of 45 000 and 150 000 MW PVDF. Details concerning the thermal history of each specimen can be found in the Experimental section. *Table 1* allows isolation of the influence of thermal history on the stress–strain response of PVDF from molecular weight effects. The rate, at which PVDF is cooled from the melt, has a significant effect on the E and σ_y values. Quenched specimens of 45 000 and 150 000 MW PVDF exhibit E values of 6.6 N mm^{-2} and 6.9 N mm^{-2}, and σ_y values of 40 N mm^{-2} and 38 N mm^{-2}, respectively. Reducing the rate of cooling to 20°C min^{-1} results in the E values of 7.8 N mm^{-2} and 7.4 N mm^{-2}, and the σ_y values of 42 N mm^{-2} and 46 N mm^{-2}. The specimens cooled at 3°C min^{-1} exhibit the E values of 9.0 N mm^{-2} and 9.0 N mm^{-2}, and the σ_y values of 52 N mm^{-2} and 53 N mm^{-2}. On the other hand, annealing specimens at 150°C increases the E values of 45 000 and

Table 1 Stress–strain data acquired from the specimens examined in this study

Thermal history	Young's modulus E (N mm^{-2})	Yield strength σ_y (N mm^{-2})
45 000 MW		
Cooled 20°C min^{-1} [a]	7.8 ± 0.2	42 ± 1.0
Quenched	6.6	40
Cooled 3°C min^{-1}	9.0	52[b]
Annealed 150°C	10.8	48
Annealed 170°C	9.1	50
150 000 MW		
Cooled 20°C min^{-1}	7.4	46
Quenched	6.9	38
Cooled 3°C min^{-1}	9.0	53
Annealed 150°C	10.2	50
Annealed 170°C	8.3	51

[a] Data from previous study[9]
[b] Strength at specimen fracture

150 000 MW PVDF to 10.8 N mm^{-2} and 10.2 N mm^{-2}, and the σ_y values to 48 N mm^{-2} and 50 N mm^{-2}. Specimens annealed at 170°C exhibit the E values of 9.1 N mm^{-2} and 8.3 N mm^{-2} and the σ_y values of 50 N mm^{-2} and 51 N mm^{-2}. According to these data, following the same thermal history, similar values for 45 000 and 150 000 MW PVDF are found. In all cases, while molecular weight plays a role in determining the stress–strain response of PVDF to uniaxial deformation, thermal history has a more significant impact.

Although the presented data show that the stress–strain response is related to the effect of thermal history on the crystalline and amorphous phases, let us identify what thermal processes are responsible for morphological features of macromolecules. For example, if the rate of cooling is slow, there is more opportunity for polymer segments to assume favourable conformations, and as a result, fewer defects are present in the crystalline phase[4]. Annealing a semicrystalline polymer also results in reduction of the crystal phase defects. This is accomplished by providing polymer chains increased freedom of motion, to assume more favourable conformations, and to minimize defects which were 'frozen' into the crystal structure during crystallization[5].

Effect of cooling rate

Cooling a polymer more slowly from the melt and annealing also affect the structure of the amorphous phase. This is achieved by reducing the number of tie molecules between crystals and chain entanglements in the amorphous phase[10]. Since tie molecules play an important role in transferring stresses through a semicrystalline network[7,11], the rate of cooling and the annealing conditions are reflected in the stress–strain data of semicrystalline polymers. As tie molecules are drawn taut between neighbouring crystals, they provide resistance to the applied stresses, which results in larger forces being required to deform the network. The number of tie molecules drawn taut in the network, and their ability to withstand the applied stresses, is reflected in the network E values, which represent the increasing resistance of the network to elastic deformations. A linear relationship between the number of tie molecules and the E value of polyethylene films has been reported[11].

Analysis of the data for PVDF presented in *Table 1*, however, suggests that there are other factors involved in the stress–strain response of PVDF. The E values of the quenched specimens of 45 000 and 150 000 MW PVDF are 6.6 N mm^{-2} and 6.9 N mm^{-2}, while the specimens cooled at 3°C min^{-1} both exhibit the E value of 9.0 N mm^{-2}. If the number of tie molecules is the only factor affecting the E values, these data are contrary to the expected behaviour. This is because, as opposed to slow cooling from the melt, quenching is expected to result in a much higher concentration of tie molecules[10]. While chain entanglements in the amorphous phase are also responsible for transferring stresses through the network, their presence does not account for the relatively high E values of the specimens cooled at 3°C min^{-1}. This is because the number of chain entanglements is also expected to be reduced by slower cooling from the melt[10].

Effect of elastic deformation

Since the higher E and σ_y values for PVDF cooled 3°C min^{-1} cannot be attributed to the number of tie molecules in the amorphous phase, let us examine how the crystalline phase thermal history may influence the stress–strain behaviour. When tie molecules are drawn taut between two crystals, they can resist applied stresses, and not necessarily unfold from the crystals, so that the distance between the crystals will remain constant. They may also unfold from their original positions in the anchoring crystals, thus resulting in the increased distance between the crystals. Whether the tie molecules resist applied stresses, or are pulled from the crystals, depend upon the number of intermolecular interactions between the segments of the tie molecule embedded in the crystal and the surrounding crystalline phase. For highly ordered crystals, a larger number of intermolecular interactions between the tie molecule segments and the crystals are anticipated. As a result, the high defect content present in the crystals of quenched polymers[5] will lead to fewer intermolecular interactions. Therefore, less force is required to pull the tie molecules from the crystals. The lower defect content in the crystals of PVDF cooled at 3°C min^{-1} results in a larger number of intermolecular interactions, and subsequently greater forces are required to unfold the tie molecules from the crystal. As shown in *Table 1*, the increased resistance of the tie molecules of PVDF cooled at 3°C min^{-1} to being pulled from their anchoring crystals is reflected in significantly higher E and σ_y values. As opposed to the specimens quenched or cooled from the melt at 20°C min^{-1}, annealing 45 000 and 150 000 MW PVDF at 150°C and 170°C results in a significant increase in the E and σ_y values. This is attributed to the reduction of the number of defects in the crystalline phase, which results in an increased number of intermolecular interactions between the crystalline phase and the tie molecule segments incorporated into the crystals.

While the stress–strain data presented in *Table 1* provide insights into the effect of thermal history on the number of tie molecules and the stresses required to unfold them from their anchoring crystals, in order to establish the influence of morphology, it is necessary to determine the crystallinity of PVDF. *Table 2* summarizes the crystallinity data of the films examined in this study. The crystallinity content ranges from 48% for quenched specimens with 45 000 and 150 000 MW, to 63 and 60% for 45 000 and 150 000 MW, cooled from the melt at 3°C min^{-1}. The crystallinity values, listed in *Table 2*, indicate that the degree of crystallinity is highly dependent upon the rate at which the specimens are cooled from the melt, and annealing the samples originally cooled from the melt at 20°C min^{-1} appears to have no effect on the degree of crystallinity.

Table 2 Crystallinity[a] of PVDF specimens (±2%)

	Crystallinity (%)				
	Thermal history				
	Cooling rate			Annealing temperature	
M_n[b]	Quenched	20°C min^{-1}	3°C min^{-1}	150°C	170°C
45 000	48	55	63	55	55
150 000	48	52	60	52	54

[a] Determined by d.s.c. measurements (Exp. section)
[b] Determined by high temperature g.p.c. (supplier)

Table 3 Desorption diffusion coefficient (D_d) ($\times 10^6$ cm^2 min^{-1}) obtained for various PVDF morphologies

	Diffusion coefficient $D_d \times 10^6$ (cm^2 min^{-1})			
	Morphological form			
	Spherulitic		Fibrous	
Thermal history	0% Strain	5% Strain	Stress-free	Stressed[a]
45 000 MW				
Cooled 20°C min^{-1} [b]	1.71 ± 0.03	1.79	1.73	1.50
Quenched	1.85	1.61	1.49	1.42
Cooled 3°C min^{-1}	1.74	1.83	[c]	[c]
Annealed 150°C	1.59	1.88	1.69	1.85
Annealed 170°C	1.27	1.63	1.95	2.27
150 000 MW				
Cooled 20°C min^{-1} [b]	1.36	1.44	1.31	1.07
Quenched	1.81	1.57	1.72	1.49
Cooled 3°C min^{-1}	1.61	1.74	1.52	1.75
Annealed 150°C	1.49	1.82	1.68	1.58
Annealed 170°C	1.18	1.23	1.96	1.97

[a] D_d measured with constant stress (≈20 N) applied to sample
[b] Data from previous study[9]
[c] Specimens fractured prior to undergoing transformation to a fibrous morphology

Having established the morphological features of PVDF as a function of MW and thermal history, let us analyse the influence of thermal history on PVDF strain-dependent permeability by examining desorption diffusion coefficients (D_d) obtained from the specimens held at constant elongations. While all experimental and theoretical background pertaining to the determination of D_d were published elsewhere[8,12], similarly to our previous studies, D_d was determined using RPA *FT*i.r. spectroscopy[9,12,13] by monitoring the rate of EtAc diffusion as a function of time. According to the relationship between the observed photoacoustic intensity (PA) and time (t)[8,9]

$$\mathrm{PA} = A \exp[x(-t^{1/2})] \quad (1)$$

or

$$\ln(\mathrm{PA}) = \ln A - xt^{1/2} \quad (1')$$

plotting the natural log of the photoacoustic intensity *versus* the square root of time should result in a straight line with a slope of x. This spectroscopically determined diffusion parameter can be quantitatively related to independently determined D_d values utilizing a calibration curve[9].

Table 3 provides D_d values obtained for spherulitic and fibrous PVDF specimens with different thermal histories. Keeping in mind PVDF morphology data presented in *Tables 1* and *2*, let us examine how polymer morphology will affect strain-dependent permeability. As seen in *Table 3*, D_d values for quenched specimens of 45 000 and 150 000 MW PVDF are 1.85×10^{-6} cm^2 min^{-1} and 1.81×10^{-6} cm^2 min^{-1}, respectively. When the specimens are subjected to 5% deformations, D_d decreases to 1.61×10^{-6} cm^2 min^{-1} and 1.57×10^{-6} cm^2 min^{-1} for 45 000 and 150 000 MW PVDF. Relative to the other specimens examined in this study, the high values of D_d are attributed to the small crystallite size expected to result from rapid cooling from the melt (*Figure 1B*), and a smaller fraction of the crystalline phase (*Table 2*) present in the quenched specimens. Reduction of the D_d values upon 5% deformation results from the presence of a large number of tie molecules, which are pulled taut by the deformation of the network. Taut tie molecules limit the mobility of amorphous phase, resulting in the decreased free volume and permeability. Thus, quenching PVDF from the melt not only reduces the overall crystallinity, but also increases the number of crystals, while decreasing their average size, and increases the number of tie molecules between them. This is schematically depicted in *Figure 1B*.

As shown in *Table 3*, permeability of the 45 000 and 150 000 MW spherulitic PVDF cooled from the melt at 3°C min^{-1}, is 1.74×10^{-6} cm^2 min^{-1} and 1.61×10^{-6} cm^2 min^{-1}, respectively. The increased permeability of these specimens, compared to the specimens cooled at 20°C min^{-1} (D_d values of 1.71×10^{-6} cm^2 min^{-1} and 1.36×10^{-6} cm^2 min^{-1} for 45 000 and 150 000 MW PVDF; *Table 3*), is somewhat surprising, because it is anticipated that the larger crystals will form for a 3°C min^{-1} cooling rate. The presence of larger crystals would mandate longer diffusion paths through the network, which should result in the decreased permeability. In view of this unexpected behaviour, let us examine the nature of the amorphous phase. Slow cooling from the melt enables more polymer chains to become disentangled during crystallization, thus resulting in a smaller number of tie molecules[10], and less hindered amorphous phase having larger free volume. Therefore, while the diffusion pathlengths are longer due to larger crystal dimensions, the permeability increase is attributed to the greater free volume of the amorphous phase. As seen in *Table 3*, 5% strain increases the permeability to 1.83×10^{-6} cm^2 min^{-1} and 1.74×10^{-6} cm^2 min^{-1} for 45 000 and 150 000 MW PVDF cooled from the melt at 3°C min^{-1}. This behaviour results from the displacement of crystals and the expansion of amorphous phase volume. With fewer tie molecules being drawn taut, the free volume, and thus the permeability of the amorphous phase, also increases.

As listed in *Table 3*, the application of 5% strain to the specimens annealed at 150°C increases the D_d values from 1.59×10^{-6} cm^2 min^{-1} and 1.49×10^{-6} cm^2 min^{-1}, to 1.88×10^{-6} cm^2 min^{-1} and 1.82×10^{-6} cm^2 min^{-1}, for 45 000 and 150 000 MW PVDF, respectively. This relatively large increase of the D_d values is surprising, because the number of tie molecules should not be significantly changed by annealing 20°C below the melting temperature. Yet, relative to the 0.08×10^{-6} cm^2 min^{-1} increase observed for the specimens cooled at 20°C min^{-1} (*Table 3*), the D_d value increases by a factor of approximately 0.3×10^{-6} cm^2 min^{-1} upon 5% deformation. This observation suggests the presence of a significantly larger increase of the free volume for the annealed specimens upon 5% deformation. In an effort to identify the origin of the D_d value changes, let us analyse the E values listed in *Table 1*. The 45 000 and 150 000 MW PVDF specimens annealed at 150°C exhibit the highest E values; specifically, 10.8 N mm^{-2} and 10.2 N mm^{-2}. They are attributed to a greater stability of crystals caused by the removal of the crystal defects during annealing[14]. More stable crystals would be expected to result in faster network deformations, because tie molecules drawn taut between two crystals are more likely to displace the crystals than be to pulled from them. When displacement of crystals occurs, the volume of the neighbouring amorphous regions increases, resulting in an increased free volume and permeability.

According to *Table 3*, annealing 45 000 and 150 000 MW PVDF at 170°C results in a decrease of the D_d values at 0% strain, from 1.71×10^{-6} cm^2 min^{-1} and 1.36×10^{-6} cm^2 min^{-1} to 1.27×10^{-6} cm^2 min^{-1} and 1.18×10^{-6} cm^2 min^{-1}, respectively. Annealing at this temperature causes a significant fraction of the original crystals to melt, allowing the formation of larger crystals, which increases the diffusion path length, and results in the observed decrease of permeability. As seen in *Table 3*, upon 5% deformation, the 150 000 MW PVDF specimen demonstrates an increase of the D_d values from 1.18×10^{-6} cm^2 min^{-1} to 1.23×10^{-6} cm^2 min^{-1}, while the permeability of the 45 000 MW PVDF specimen increases from 1.27×10^{-6} cm^2 min^{-1} to 1.63×10^{-6} cm^2 min^{-1}. Relative to the 150 000 MW, the 45 000 MW PVDF has fewer tie molecules because the number of tie molecules is proportional to molecular weight[7]. During deformation, the free volume of the network is increased by the expansion of the amorphous phase for specimens of both molecular weights. The larger number of tie molecules drawn taut in the 150 000 MW PVDF specimens restricts the motion of the amorphous phase, resulting in a smaller increase of free volume.

Morphology and permeability

As described previously[9], upon uniaxial deformation, PVDF morphology changes from spherulitic to fibrous forms. The spherulitic morphology, schematically depicted in *Figure 1*, is composed of randomly oriented crystals, separated by regions of amorphous polymer. The fibrous morphology, shown schematically in *Figure 2*, contains many microfibrils, which are composed of alternating regions of crystalline and amorphous polymer. Let us now determine if further insights into the morphology of these PVDF samples may be gained from the permeability data of their fibrous polymorphs. During transformation from spherulitic to fibrous

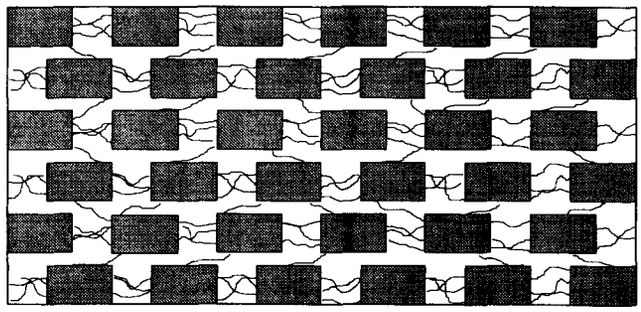

Figure 2 Schematic of the fibrous semicrystalline morphology

morphology, tie molecules transfer stresses through a polymer network[7]. After development of sufficient stresses, the crystals present in the original network are destroyed as tie molecules are pulled from them. As the polymer chains become aligned in the strain direction, recrystallization occurs, and the nature of the network dictates that the crystalline phase of the fibrous morphology is composed primarily of material which was crystalline in the spherulitic form. The regular chain structure of the polymer chains and the chain segments crystallized during cooling from the melt makes their recrystallization highly feasible. Conversely, amorphous regions are comprised of chain entanglements, tie molecules, and defects in chain structure, which are likely to remain in the amorphous state upon transformation of the network to the fibrous form. Therefore, by examining the permeability of fibrous polymorphs, it may be possible to gain further insight into the number of tie molecules bridging the amorphous phase.

According to *Table 3*, fibrous 45 000 and 150 000 MW PVDF specimens, crystallized by quenching from the melt, exhibit a decrease of the D_d values from 1.73×10^{-6} cm^2 min^{-1} and 1.72×10^{-6} cm^2 min^{-1}, to 1.50×10^{-6} cm^2 min^{-1} and 1.49×10^{-6} cm^2 min^{-1}, respectively, when they experience approximately 20 N of applied stress. As discussed above, the rapid crystallization of these specimens is expected to result in the formation of many tie molecules. Drawing these tie molecules taut restricts the mobility of other polymer chains in the amorphous phase, thereby reducing free volume and permeability. When stresses are applied (*Table 3*), the D_d values of fibrous specimens of 45 000 and 150 000 MW PVDF cooled from the melt at 20°C min^{-1} decrease from 1.73×10^{-6} cm^2 min^{-1} and 1.31×10^{-6} cm^2 min^{-1} to 1.50×10^{-6} cm^2 min^{-1} and 1.07×10^{-6} cm^2 min^{-1}, respectively. This observation is again attributed to the presence of many tie molecules being drawn taut, and restricting the mobility of the amorphous phase.

Table 3 indicates that, upon application of 20 N, the permeability of fibrous 150 000 MW PVDF cooled from the melt at a rate of 3°C min^{-1} increases from 1.52×10^{-6} cm^2 min^{-1} to 1.75×10^{-6} cm^2 min^{-1}. When the amorphous phase volume increases as a result of deformation, the decreased number of tie molecules, which result from slowly cooling the network from the melt[10], is insufficient to limit mobility of amorphous phase chains. Increased free volume of the amorphous phase, without the restrictions of taut tie molecules, results in the increased permeability.

The reduction in the number of tie molecules is of greater significance for the 45 000 MW polymer. When elongated, the film fractures before undergoing transformation to the fibrous form. The relatively short chain

length enables the polymer chains to disentangle to a greater degree during crystallization, resulting in fewer tie molecules between crystals. There are too few tie molecules present to withstand the stress required to transform the network to a fibrous morphology. Therefore, as stresses increase during deformation, the local stress on each tie molecule is such that it causes chain rupture and failure of the film.

As seen in *Table 3*, the permeability of the fibrous 45 000 MW PVDF specimens annealed at 150°C increases from 1.69×10^{-6} cm^2 min^{-1} to 1.85×10^{-6} cm^2 min^{-1} upon the application of 20 N. The application of equal force to a fibrous specimen of 150 000 MW PVDF annealed at 150°C decreases the D_d value from 1.68×10^{-6} cm^2 min^{-1} to 1.58×10^{-6} cm^2 min^{-1}. The different responses of the networks to the applied stresses are once again related to the greater number of tie molecules in the 150 000 MW specimen, which limit the free volume of the amorphous phase.

The D_d values obtained for the fibrous 45 000 and 150 000 MW specimens annealed at 170°C in the stress free state are 1.95×10^{-6} cm^2 min^{-1} and 1.96×10^{-6} cm^2 min^{-1}, respectively (*Table 3*). The increase of permeability in the stress free state, relative to the fibrous samples annealed at 150°C (D_d equal to 1.69×10^{-6} cm^2 min^{-1} and 1.68×10^{-6} cm^2 min^{-1} for 45 000 and 150 000 MW PVDF, respectively, *Table 3*), contrasts with the significantly lower permeability observed for the corresponding spherulitic specimens annealed at 170°C (D_d values of 1.27×10^{-6} cm^2 min^{-1} and 1.18×10^{-6} cm^2 min^{-1} for 45 000 and 150 000 MW PVDF, respectively, as opposed to 1.59×10^{-6} cm^2 min^{-1} and 1.49×10^{-6} cm^2 min^{-1} for 45 000 and 150 000 MW PVDF annealed at 150°C). The lower permeability of the spherulitic specimens annealed at 170°C is attributed to the formation of significantly larger crystals, which increase the diffusion path length, and therefore, reduces permeability. As described above, the crystals present in the spherulitic morphology are destroyed during transformation to the fibrous state. The highly disordered state achieved during the spherulitic to fibrous transformation results in the formation of smaller crystals when recrystallization occurs in the fibrous form.[11] Since annealing at 170°C is expected to reduce the number of

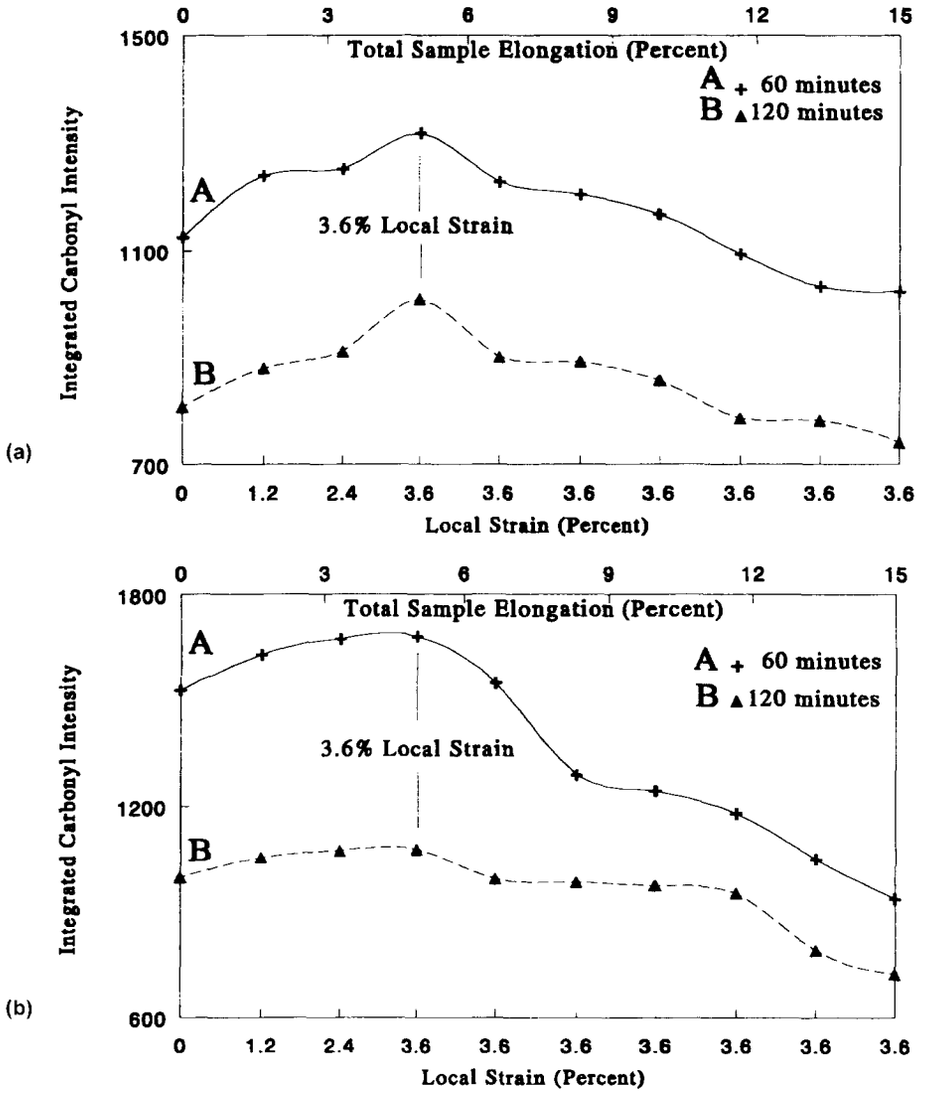

Figure 3 Integrated intensity of the band at 1768 cm^{-1} plotted as a function of elongation. Data obtained from 45 000 MW (a) and 150 000 MW PVDF (b), quenched from the melt, experiencing elastic deformation. Curves A and B represent films dried 60 and 120 min prior to elongation, respectively

tie molecules to a greater extent than annealing at 150°C[5], the small crystals of the fibrous state are connected by a smaller number of tie molecules, which restrict the mobility of the amorphous phase chains to a smaller extent, thus accounting for the higher permeability of the fibrous polymorphs of specimens annealed at 170°C.

The application of 20 N stress to the fibrous PVDF annealed at 170°C results in an increase of the D_d values from 1.95×10^{-6} cm^2 min^{-1} to 2.27×10^{-6} cm^2 min^{-1} for 45 000 MW PVDF. At the same time, the D_d values for 150 000 MW PVDF remain almost unchanged before and after the application of stresses (1.95×10^{-6} cm^2 min^{-1} and 1.96×10^{-6} cm^2 min^{-1}). This behaviour is attributed to the fact that the larger number of tie molecules in the 150 000 MW specimen reduces the mobility of the amorphous phase chains, thus offsetting the increase of free volume, which results from expansions of the amorphous phase.

While the permeability data presented in *Table 3* provides information on the morphology of the specimens examined in this study, including response to 5% deformation, the primary objective of this study is the determination of how PVDF morphologies generated by various thermal treatments respond to deformations. Therefore, permeability measurements were conducted, using the RPA *FT*i.r. experimental setup[8,12], as a function of elongation for each of the specimens listed in *Table 3*. As noted previously[9], when PVDF is elongated, the entire film experiences deformation during the first stage of deformation. After the yield point is reached, however, one region of the film thins and narrows, as it transforms from a spherulitic to a fibrous morphology, forming the plastically deformed 'neck'. Beyond the yield point, the degree of strain becomes constant in the regions not undergoing transformation to the fibrous form. Since deformations that occur prior to the spherulitic–fibrous transformation is recoverable, these regions are referred to as the elastically deformed regions. In contrast, those regions which experience the transformation to a fibrous morphology are referred to as plastically deformed. Thus, in order to understand the response of the specimen to uniaxial elongations, both elastically and plastically deformed regions of the sample will be examined.

As noted in the Experimental section, each specimen

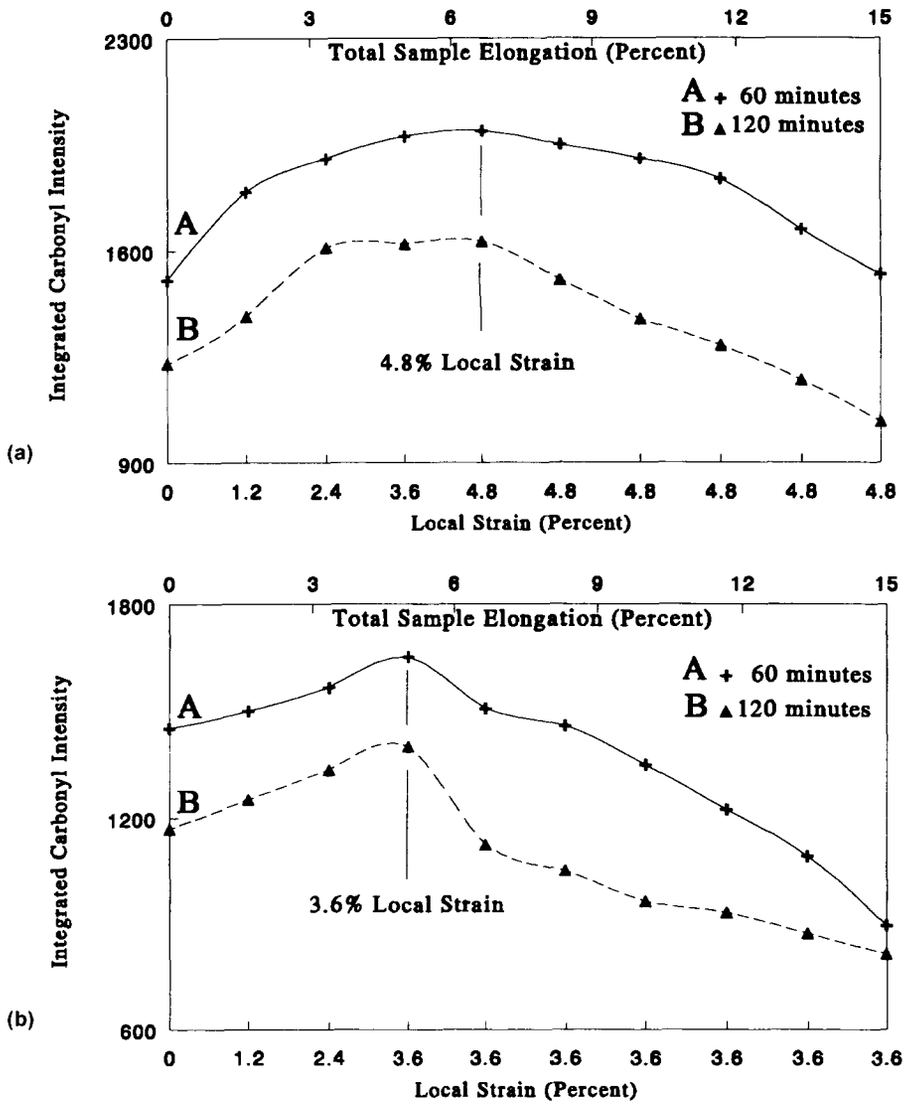

Figure 4 Integrated intensity of the band at 1768 cm^{-1} plotted as a function of elongation. Data obtained from 45 000 MW (a) and 150 000 MW PVDF (b), cooled from the melt at 3°C min^{-1}, experiencing elastic deformation. Curves A and B represent films dried 60 and 120 min prior to elongation, respectively

contains a notch which is half the width of the remainder of the film. Therefore, this region experiences twice the stresses per cross-sectional area. Recalling that the taut tie molecules between crystals are responsible for transferring stresses through a semicrystalline polymer[7], it is apparent that, the greater the stresses experienced by a polymer, the larger the number of tie molecules which must be drawn taut. Thus, relative to the elastically deformed regions, the plastically deformed regions will contain approximately twice the number of taut tie molecules. In order for a larger number of tie molecules to be drawn taut, the plastically deforming region must experience a higher degree of deformation, as demonstrated in the lower x axis of *Figures 3–10*, which represents the degree of local strain.

With this in mind, let us go back to the main theme and focus on the permeability measurements obtained using RPA *FT* i.r. spectroscopy. The curves illustrated in *Figures 3–10* represent the integrated intensities of the infra-red band at 1768 cm^{-1}, attributed to the carbonyl of vapour phase EtAc, recorded as a function of strain. As we recall, EtAc is used as the diffusant molecule in PVDF, and its concentration in the gas phase reflects the rate at which EtAc diffuses out of the PVDF network. Curves A and B in all figures were obtained from specimens allowed to dry at 25°C, prior to monitoring permeability under various strains, for 60 and 120 min, respectively. As described previously[9], the concentration of EtAc in the PVDF specimens decreases as the experiment proceeds. The utilization of two periods of EtAc evaporation prior to monitoring strain dependent diffusion ensures that the observed intensity changes are strain dependent and not due to changing EtAc concentrations. Following low degrees of deformation, strain is constant in the elastically deformed regions, and increases continually in the plastically deformed region. For that reason, the degree of deformation is presented on two axis in *Figures 3–10*. The top axis provides the degree of strain experienced by the entire sample, while the bottom axis denotes the extent of deformation in the region of the film being examined. Each data point presented in *Figures 3–10* represents the average of at least three measurements.

Before we examine the effect of cooling rate and annealing on PVDFs response to elastic deformation, let us review the results obtained from PVDF specimens

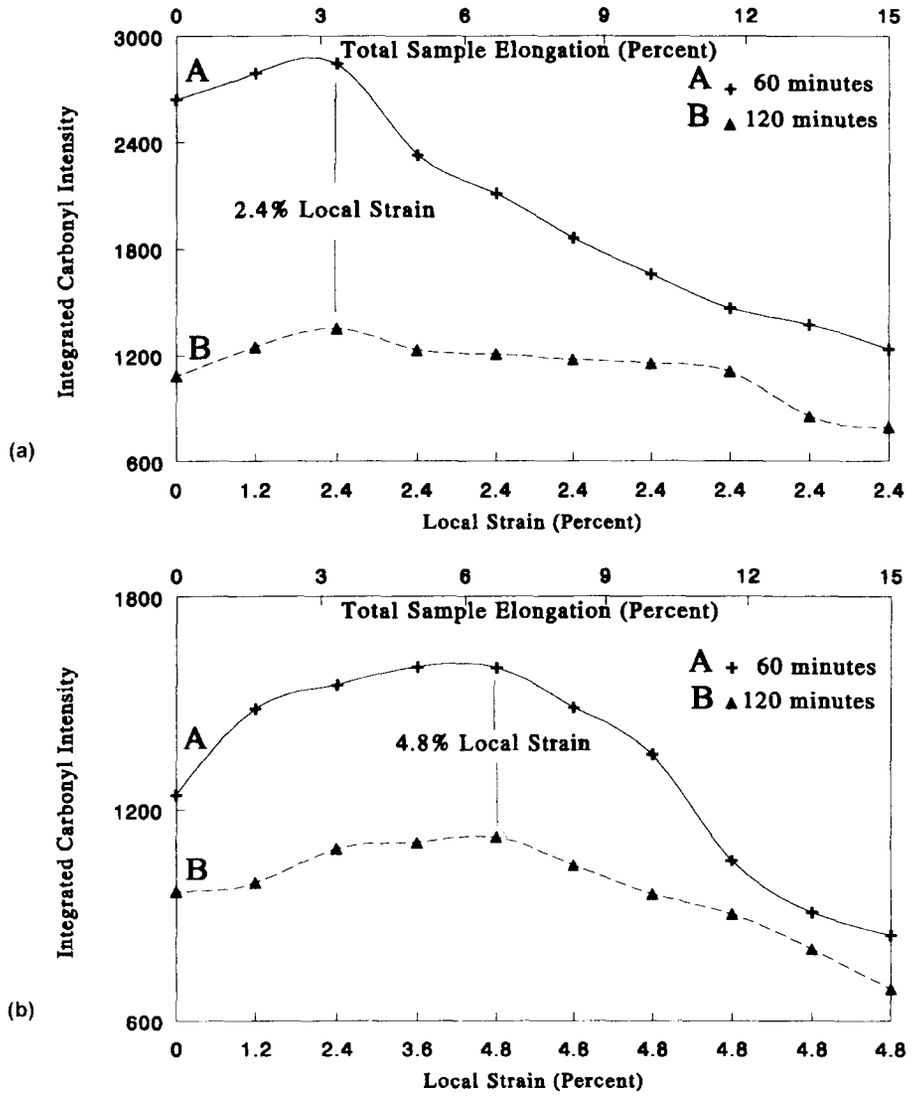

Figure 5 Integrated intensity of the band at 1768 cm^{-1} plotted as a function of elongation. Data obtained from 45 000 MW (a) and 150 000 MW PVDF (b), cooled from the melt at 20°C min^{-1} and annealed at 150°C for 18 h, experiencing elastic deformation. Curves A and B represent films dried 60 and 120 min prior to elongation, respectively

cooled from the melt at 20°C min^{-1}[9]. The 45 000 and 150 000 MW PVDF specimens, cooled from the melt at 20°C min^{-1}, exhibit increases in permeability up to 4.8% local strain. During the first stages of elongation, the concentration of EtAc observed in the RPA cell is enhanced, indicating enhanced diffusion of EtAc out of PVDF. The enhanced transport properties are attributed to the increased amorphous phase free volume. The increased free volume results from crystals interfering with the lateral contraction of the film, which causes volume expansions[9]. The specific volume reaches a maximum in the elastically deformed regions of the specimen when the degree of strain becomes constant. With no further increase in free volume, the rate of EtAc exhudation should become dependent upon its concentration within the film, and decrease with time.

Keeping in mind morphology data listed in *Tables 1, 2* and *3*, let us now examine how thermal treatment modifies the response of PVDF to elastic deformations. As seen in *Figures 3a* and *b*, 45 000 and 150 000 MW PVDF quenched from the melt exhibit increased permeability, up to 3.6% local strain. This behaviour is not observed for the specimens cooled at 20°C min^{-1}, which display maximum permeability at 4.8% local strain. The attainment of maximum permeability at a lower degree of strain for the quenched specimens is attributed to the presence of a large number of tie molecules. With more tie molecules in the network, a lower degree of deformation is required for sufficient tie molecules to be drawn taut in the elastically deformed region in order to provide resistance to the stresses transferred through plastically deformed regions. Therefore, deformations of elastically deformed regions reach a maximum at a lower degree of strain, resulting in all further deformations occurring in the plastically deformed region.

Figures 4a and *b* display the analogous diffusion data for elastically deformed region of 45 000 and 150 000 MW PVDF films cooled at 3°C min^{-1}. The rate of EtAc exhudation appears to increase up to 4.8% and 3.6% local strains. The linear dependence of the number of tie molecules on molecular weight[7] results in the 150 000 MW PVDF network containing more tie molecules. Therefore, a lower degree of strain needs to be achieved for a sufficient number of tie molecules to be drawn taut in the

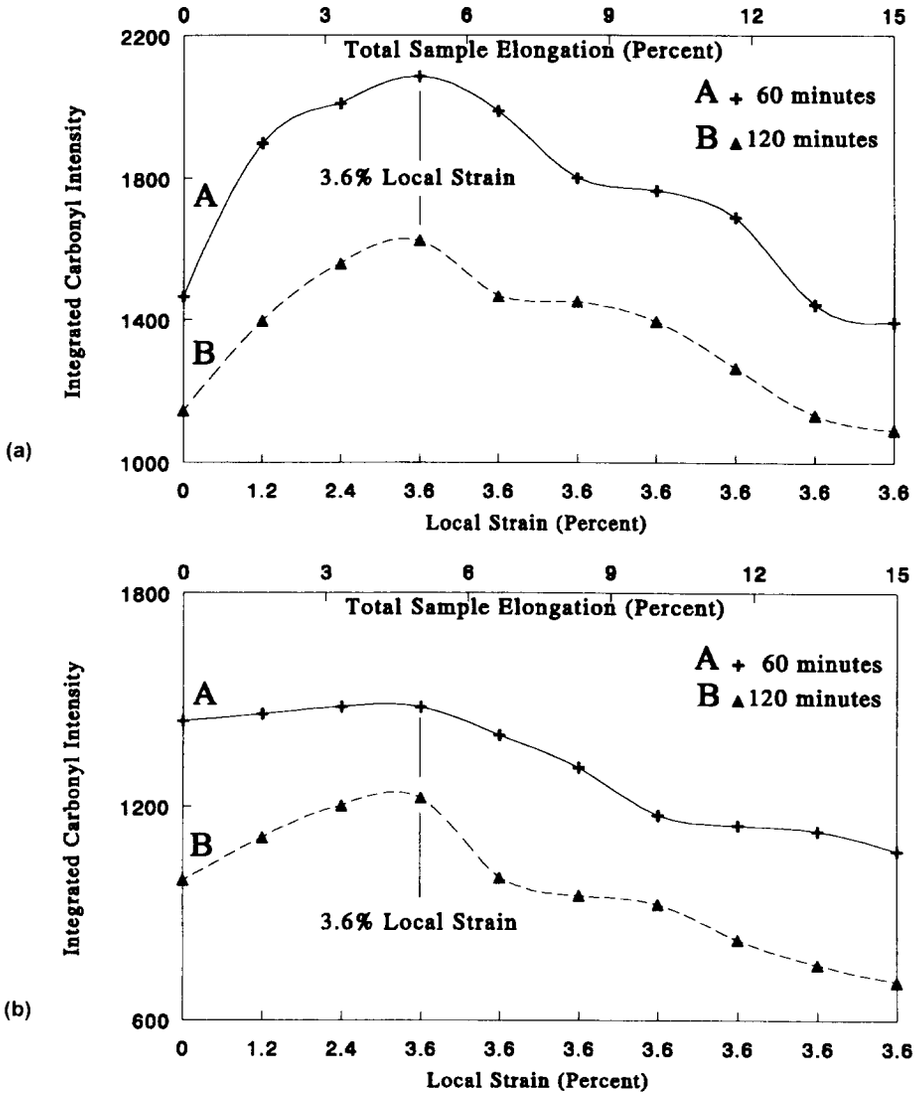

Figure 6 Integrated intensity of the band at 1768 cm^{-1} plotted as a function of elongation. Data obtained from 45 000 MW (a) and 150 000 MW PVDF (b), cooled from the melt at 20°C min^{-1} and annealed at 170°C for 18 h, experiencing elastic deformation. Curves A and B represent films dried 60 and 120 min prior to elongation, respectively

elastically deformed regions to cause plastic deformation in the narrowed region of the specimen. The maximum permeability occurs at 3.6% and 4.8% local strain for 150 000 MW PVDF cooled from the melt at 3°C min^{-1} and 20°C min^{-1}, respectively. This observation is surprising if one considers only the number of tie molecules in the network. After all, relative to the specimens cooled at faster rates, slow crystallization results in a smaller number of tie molecules[10]. It would be anticipated that a smaller number of tie molecules would result in a slower build up of stresses in the film, since fewer are drawn taut during each step of deformation. As seen in *Table 1*, the E value of 9.0 N mm^{-2} for the specimens cooled at 3°C min^{-1} is actually higher than that of films cooled from the melt at 20°C min^{-1} ($E = 7.4$ N mm^{-2}). The higher modulus values are attributed to the fact that the slow crystallization process results in the crystals having fewer defects and greater stability. Higher stresses are therefore required to pull the tie molecules from the crystals. Thus, the tie molecules drawn taut in the early stages of deformation are more likely to resist applied stresses and are less likely to be pulled from the crystals. This results in a lower degree of deformation in the elastically deformed region for sufficient tie molecules to be drawn taut to resist the stresses transferred through the plastically deformed region.

The data in *Figures 5a* and *b* present the relative permeability plotted as a function of elongation in the elastically deformed region for 45 000 and 150 000 MW PVDF specimens annealed at 150°C. 45 000 MW PVDF, curves A and B of *Figure 5*, exhibit a maximum permeability at 2.4% local strain. The early onset of the maximum permeability is attributed to the response of this low MW polymer to annealing. Annealing at 150°C results in the melting of the smallest, least stable crystals and recrystallization of their component material into larger crystals[14]. The average crystal size achieved by this polymer, when cooled from the melt at 20°C min^{-1}, is anticipated to be smaller than that obtained from higher molecular weights crystallized under the same conditions. This is reflected in its relatively high permeability values at 0% strain ($D_d = 1.71 \times 10^{-6}$ cm^2 min^{-1} as opposed to 1.36×10^{-6} cm^2 min^{-1} for 150 000 MW PVDF cooled from the melt at 20°C min^{-1}). Therefore, redistribution of the crystalline phase into fewer, but larger crystals is more likely to

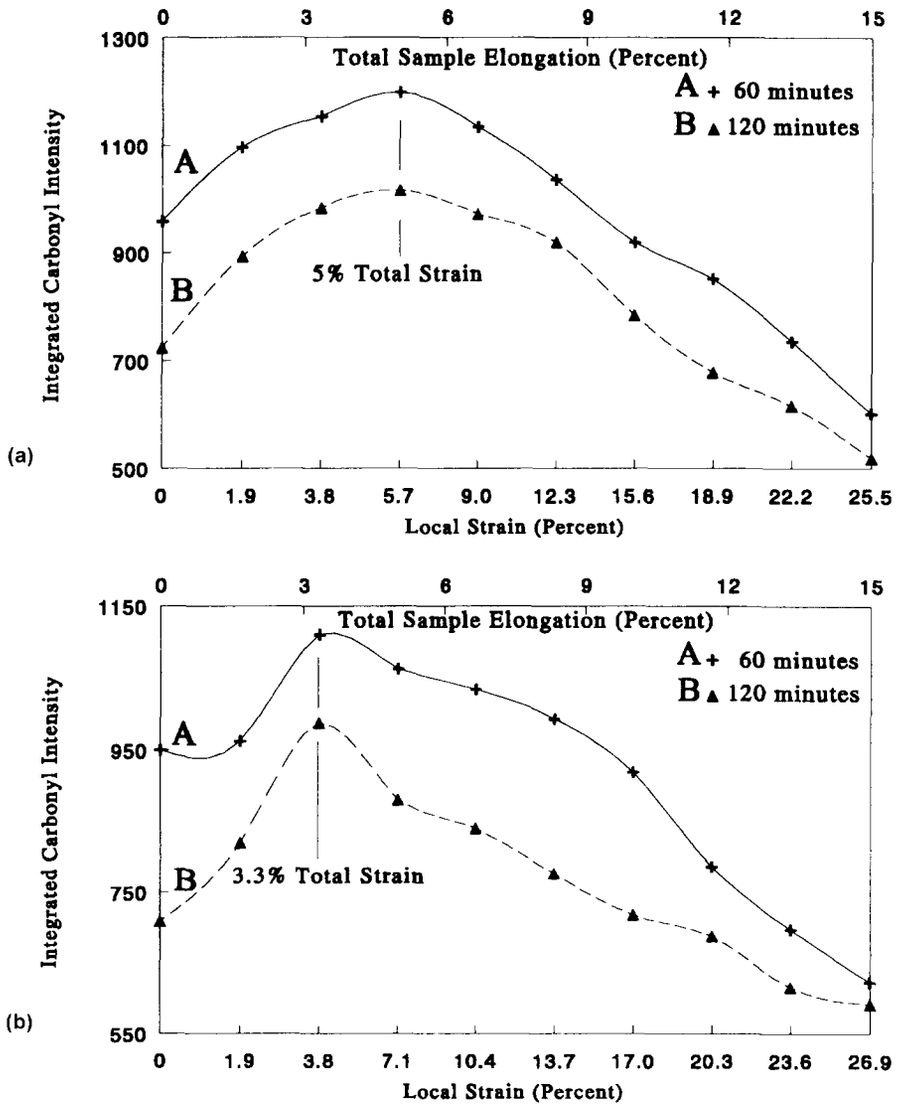

Figure 7 Integrated intensity of the band at 1768 cm^{-1} plotted as a function of elongation. Data obtained from 45 000 MW (a) and 150 000 MW PVDF (b), quenched from the melt, experiencing plastic deformation. Curves A and B represent films dried 60 and 120 min prior to elongation, respectively

result in the significant changes of the crystal size than for the higher molecular weight analogue. While annealing at 150°C melts the least stable crystals, the majority are expected to remain intact. Thus, the tie molecules present between them will not be removed by annealing at this temperature. Therefore, annealing 45 000 MW PVDF at 150°C results in the enlargement of the crystals without substantially decreasing the number of tie molecules connecting them. Annealing PVDF below its melting point also reduces the number of defects present in the crystals[14]. Thus, a combination of tie molecules and more stable crystals results in the high E value of 10.8 N mm^{-2} (*Table 1*) detected for this specimen. As a consequence, a lower degree of deformation is required to draw sufficient tie molecules taut in the elastically deformed region to induce plastic deformations.

Annealing at 150°C has a less significant effect on the semicrystalline network of the 150 000 MW PVDF. This is demonstrated by the maximum elongation and permeability of the elastically deformed region at 4.8% local strain (*Figure 5b*), which is the same degree of extension at which the maxima are observed prior to annealing[9]. Relative to the crystals of 45 000 MW PVDF, the larger crystals formed by 150 000 MW PVDF are more stable, and less likely to melt at 150°C. Therefore, in comparison to the unannealed specimens, no change in the network's response to deformations is detected.

Figures 6a and *b* present the rate of EtAc exhudation as a function of elastic deformation for 45 000 and 150 000 MW PVDF annealed at 170°C. Both 45 000 and 150 000 MW PVDF exhibit a maximum rate of exhudation at 3.6% local strain. The appearance of maximum permeability at 4.8 and 3.6% local strain, before and after annealing at 170°C, is once again attributed to the increased stability of the crystalline phase, which results from the removal of crystal defects by annealing. The increased stability of the crystals is reflected in the σ_y values. The 45 000 and 150 000 MW PVDF exhibit σ_y values of 50 and 50.6 N mm^{-2}, which are significantly higher than the σ_y values of 42 and 46 N mm^{-2} prior to annealing (*Table 1*). Increased crystal stability results in the tie molecules being less likely to be pulled from their anchoring crystals, and stresses building more rapidly in the annealed specimens, which exhibit E values of 9.1

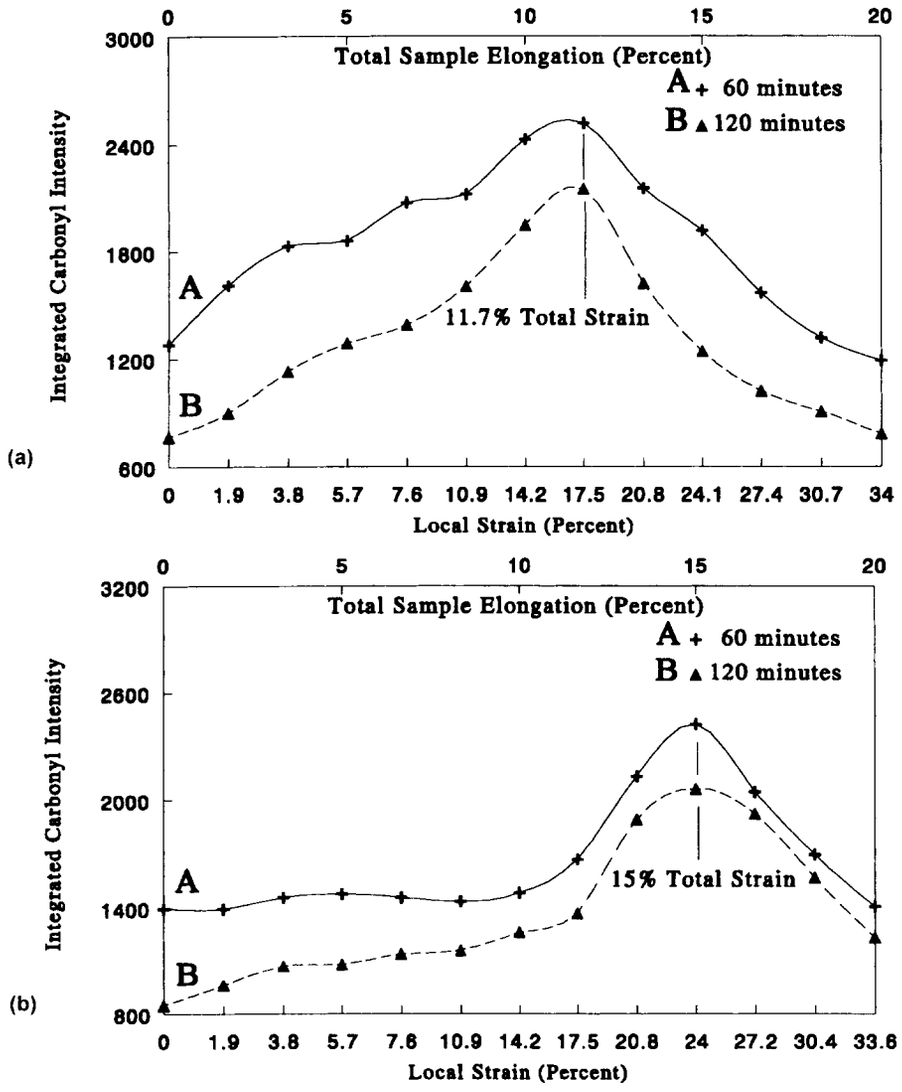

Figure 8 Integrated intensity of the band at 1768 cm^{-1} plotted as a function of elongation. Data obtained from 45 000 MW (a) and 150 000 MW PVDF (b), cooled from the melt at 3°C min^{-1}, experiencing plastic deformation. Curves A and B represent films dried 60 and 120 min prior to elongation, respectively

and 8.3 N mm^{-2}. In contrast, the E values for 45 000 and 150 000 MW PVDF prior to annealing are 7.8 and 7.4 N mm^{-2}, respectively. Therefore, sufficient amounts of tie molecules are drawn taut at 3.6% local strain in the elastically deformed region to cause plastic deformations in the narrowed region of the specimen.

One other notable observation in *Figures 6a* and *b* is that, relative to the 150 000 MW PVDF, the 45 000 MW PVDF experiences a significantly larger increase in permeability up to 3.6% local strain. This increase is in agreement with the D_d value changes observed while going from 0 to 5% deformations. While 150 000 MW PVDF shows an increase of the D_d values from 1.18×10^{-6} cm^2 min^{-1} to 1.23×10^{-6} cm^2 min^{-1}, the permeability of 45 000 MW PVDF increases from 1.27×10^{-6} cm^2 min^{-1} to 1.63×10^{-6} cm^2 min^{-1} (*Table 3*). The larger number of tie molecules present in the network of the 150 000 MW PVDF results in the restricted mobility of the amorphous phase chains when stresses are applied. The loss of amorphous phase mobility to taut tie molecules partially cancels the effect of increased free volume brought about by the increase of the amorphous phase volume, and limits the D_d increase.

Effect of plastic deformation

Having examined the effect of elastic deformation on PVDF permeability, we now turn to the plastically deformed region. *Figures 7a* and *b* present the strain dependent permeability for the plastically deformed region of the 45 000 and 150 000 MW PVDF quenched from the melt. Curves A and B of *Figure 7* indicate that the permeability of 45 000 MW PVDF increases up to 5.7% local strain, and then steadily declines. *Figure 7b* illustrates that the maximum permeability of 150 000 MW PVDF is attained at 3.8% local strain. The increased permeability, at the early stages of deformation, is consistent with an increase of the amorphous phase free volume, which results from the volume expansions, as described for the elastically deformed region. A surprising feature of the data presented in *Figures 7a* and *b* is the appearance of the maximum rate of EtAc exhudation prior to the formation of voids, which occurs at approximately 12.3% local strain for both samples. Voids in a network provide unobstructed diffusion pathways, and their presence results in an enhanced permeability[8,9].

The observation of maximum permeability before the

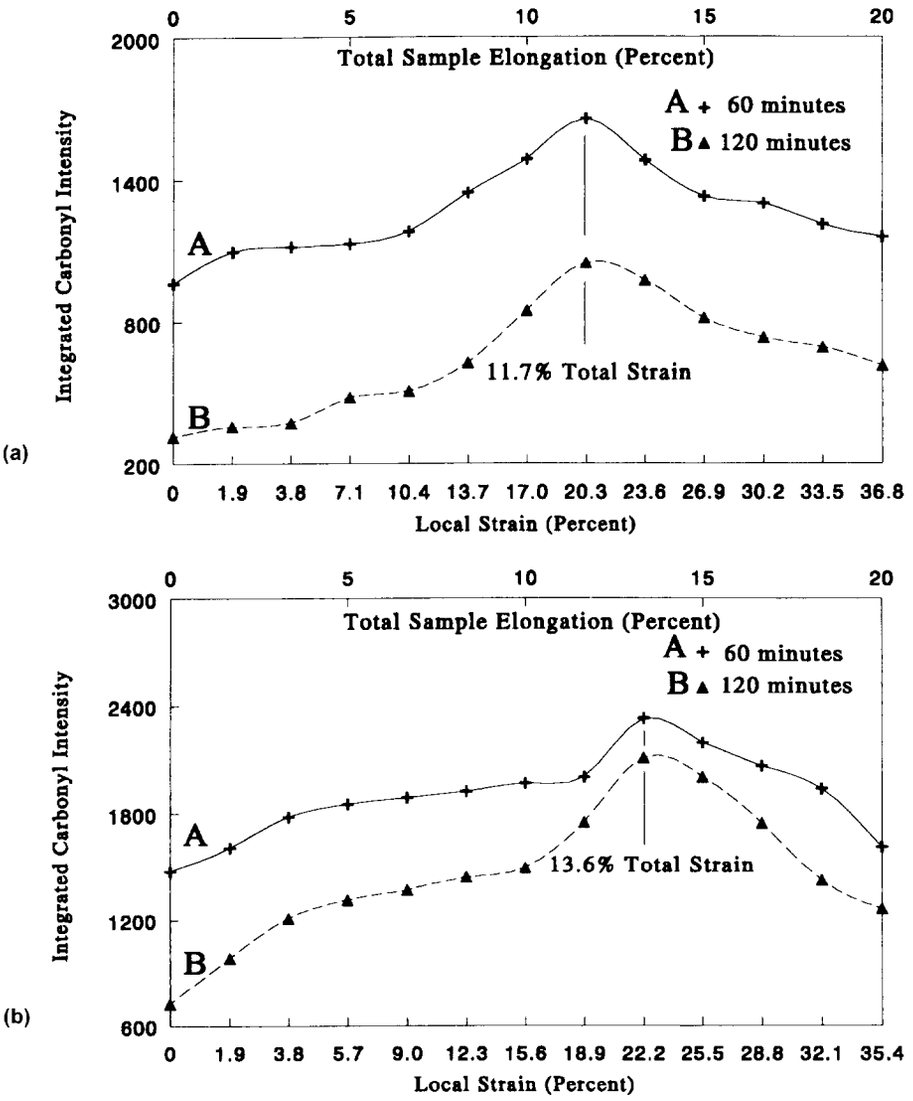

Figure 9 Integrated intensity of the band at 1768 cm^{-1} plotted as a function of elongation. Data obtained from 45 000 MW (a) and 150 000 MW PVDF (b), cooled from the melt at 20 °C min^{-1} and annealed at 150 °C for 18 h, experiencing plastic deformation. Curves A and B represent films dried 60 and 120 min prior to elongation respectively

appearance of voids is attributed to low crystallinity content (48%, *Table 2*) and a small crystal size. As opposed to slow crystallization, the rapid crystallization, which occurs upon quenching the specimen, yields smaller, although less perfectly formed crystals. When the network is deformed, less stress is required to pull taut tie molecules from the imperfectly formed crystals. Therefore, lower degrees of stress are transferred through the film, thus reducing the number of crystals which are displaced sufficiently to induce the void formation. Due to the formation of fewer voids, the onset of void formation will have a less significant impact on permeability for quenched specimens than for the specimens cooled at slower rates. The latter will have a large number of voids formed during the spherulitic to fibrous transition. The permeability of the quenched specimen also plays a role in determining the degree of strain at which the maximum rate of EtAc exhudation is observed. Relative to the other specimens, smaller crystals and lower crystallinity result in a high permeability at 0% strain ($D_d = 1.85 \times 10^{-6}$ cm^2 min^{-1} for 45 000 and 150 000 MW PVDF). As the experiment proceeds from 0 to 12.3% local strain, the EtAc concentration is expected to decrease more rapidly for quenched, spherulitic PVDF specimens than for the specimens cooled at slower rates from the melt. The latter exhibit lower permeabilities (*Table 3*). The formation of fewer voids, combined with a significantly reduced EtAc concentration, results in a failure of the void formation to cause an increase in the EtAc exhudation at 12.3% local strain.

Curves A and B of *Figures 8a* and *b* represent the strain dependent permeability of the plastically deformed regions for the 45 000 and 150 000 MW PVDF cooled from the melt at a rate of 3°C min^{-1}. As seen in *Figure 8*, up to 11.7% total strain, the rate of EtAc exhudation from 45 000 MW experiences significant increases with elongation. *Figure 8b* demonstrates that, for the 150 000 MW PVDF, a slow increase of EtAc exhudation up to 11.7% total strain, is observed. This is followed by a rapid increase of permeability, up to 15% total strain. The rapid increase in permeability at low degrees of strain for the 45 000 MW specimens is attributed to the fact that there is a small number of tie molecules in the network. As discussed earlier, the number of tie molecules in the network is significantly reduced by slow crystallization.

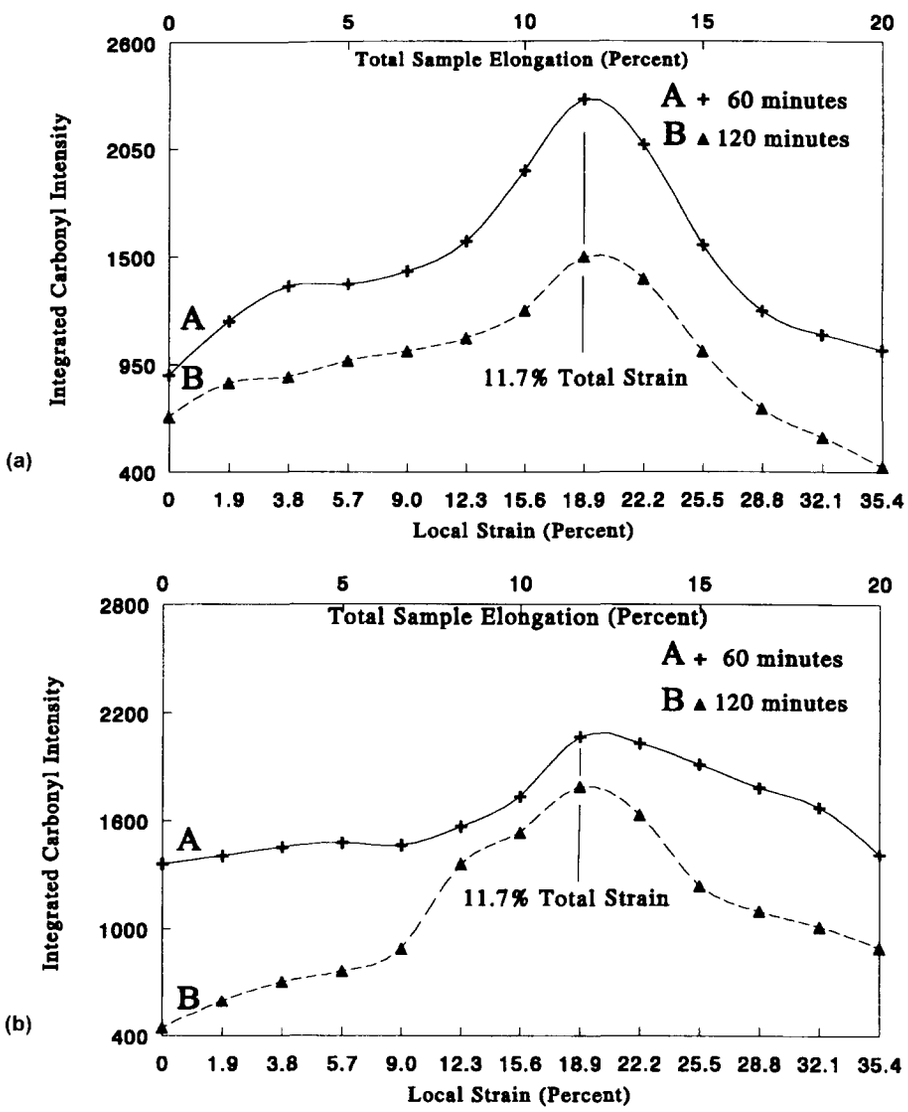

Figure 10 Integrated intensity of the band at 1768 cm^{-1} plotted as a function of elongation. Data obtained from 45 000 MW (a) and 150 000 MW PVDF (b), cooled from the melt at 20°C min^{-1} and annealed at 170°C for 18 h, experiencing plastic deformation. Curves A and B represent films dried 60 and 120 min prior to elongation, respectively

This is suggested by the relatively high permeability of the network at 5% strain ($D_d = 1.83 \times 10^{-6}$ cm^2 min^{-1}, *Table 3*), and the fracture of the specimens prior to the formation of fibrous morphology. Therefore, as the volume of the amorphous phase increases during deformation, there is a smaller number of tie molecules drawn taut to limit the mobility of amorphous phase material. Increased volume, without the hindrance of taut tie molecules, results in a significant increase of the permeability for the 45 000 MW specimen during the early stages of deformation. The presence of a greater number of tie molecules accounts for the slower increase in permeability observed at low degrees of strain for the 150 000 MW PVDF. As the film deforms, more tie molecules are drawn taut, which limits the mobility of the amorphous phase, and reduces the free volume. The significant increase in permeability, between 11.7 and 15% local strain, corresponds to the void formation in the plastically deformed region.

Several factors should be considered when examining the degree of strain at which the maximum rate of EtAc exhudation is observed. Relative to cooling at 20°C min^{-1}, cooling at a rate of 3°C min^{-1} is expected to result in the formation of larger crystals, with fewer defects, and a smaller number of tie molecules connecting them. The rate of maximum EtAc exhudation for 45 000 MW PVDF, cooled from the melt at 3°C min^{-1} and 20°C min^{-1}, is detected at 11.75 and 10% total strain, respectively. However, the maximum rate of EtAc exhudation for 150 000 MW PVDF specimens cooled from the melt at 3°C min^{-1} and 20°C min^{-1}, is detected at 15% and 11.7% total strain, respectively. Recalling that, relative to a network cooled at 3°C min^{-1} [5], cooling at a rate of 20°C min^{-1} is anticipated to result in the formation of smaller crystals, these observations agree with our earlier findings[9], which suggested that the presence of larger crystals reduces the rate at which crazing spreads through the plastically deformed region of PVDF. For the specimens with the same crystalline content, reduced crystallite size results in a larger number of crystals randomly distributed in a unit volume. Thus, when the smaller PVDF crystals are displaced, and form microcracks, they impinge upon neighbouring crystals after smaller displacements. This, in turn, hinders the expansion of cracks. Thus, further elongation results in the formation of new microcracks, and accelerates the rate at which crazing spreads through the plastically deformed region. The appearance of maximum permeability at 11.7 and 15% total strain for 45 000 and 150 000 MW PVDF cooled at 3°C min^{-1}, vs 10 and 11.7% total strain for specimens cooled at 20°C min^{-1}, is attributed to an increase of the crystallite size, obtained by cooling the specimens from the melt at lower rates, resulting in a slower spread of crazing through the network.

The curves presented in *Figures 9a* and *b* were obtained from 45 000 and 150 000 MW PVDF annealed at 150°C. They demonstrate maxima of the EtAc exhudation rates for 45 000 MW PVDF at 11.7% total strain (*Figure 9a*), and 13.3% total strain for 150 000 MW (*Figure 9b*). Relative to the specimens cooled from the melt at 20°C min^{-1}, annealing is anticipated to increase the average crystal size[14,15]. Due to the mechanism described above, the increase of average crystal size results in the maximum permeability detected at a higher degree of deformations.

Figures 10a and *b* present relative permeability values plotted as a function of strain for 45 000 and 150 000 MW PVDF specimens which were annealed at 170°C. For both specimens, the maximum rate of EtAc exhudation is observed at 11.7% total strain. As described above, annealing is expected to increase the average crystal size. The presence of larger crystals once again accounts for the shift of the location of maximum permeability for 45 000 MW PVDF, from 10% total strain prior to annealing, to 11.7%. However, 150 000 MW PVDF displays maximum permeability at 11.7% total strain before and after annealing at 170°C. The presence of larger crystals is indicated by the reduction of the 0% strain D_d values from 1.36×10^{-6} cm^2 min^{-1} to 1.18×10^{-6} cm^2 min^{-1} upon annealing at 170°C (*Table 3*). Appearance of the maximum permeability at the same degree of strain, before and after annealing, is attributed to the increased stability of the crystals produced by annealing. When microcracks form between neighbouring crystals, the tie molecules bridge them. If the tie molecules are pulled from the crystals, the cracks continue to expand. If they resist unfolding from the crystals, the cracks do not expand, and further elongation results in the formation of new cracks. Thus, the increased stability of crystals, resulting from a decreased number of crystal defects, requires that greater stresses are applied to draw the tie molecules from them. Therefore, the tie molecules resist expansions of previously formed cracks, which account for the increased rates of crazing in the plastically deformed regions.

CONCLUSIONS

Sensitivity of photoacoustic infra-red spectroscopy to gas phase species, as well as its versatility to simultaneous stress–strain measurements, make RPA *FT* i.r. spectroscopy an ideally suited tool for the studies of permeability as a function of external stresses. While increased PVDF permeability observed during the early stages of elastic deformation is attributed to the increased free volume of the amorphous component of the network, the increase of network permeability at the latter stages occurs when microcracks and voids are formed, and the network undergoes transition from spherulitic to fibrous morphology.

Although molecular weight of PVDF plays a role in the network permeability, the effects of thermal history dominate the permeability changes. Variations in network permeability at 0% strain are primarily attributed to the crystalline phase content of the network, and the size of the individual crystals. However, upon application of stresses, the number of tie molecules, and their resistance to being pulled from their anchoring crystals dominate the permeability of the network. Stress–strain responses of PVDF indicate that the resistance of the tie molecules to being pulled from their anchoring crystals increases at slower cooling rates, and after annealing.

ACKNOWLEDGEMENT

Acknowledgement is made to the donors of The Petroleum Research Fund, administered by the ACS, for support of this research (ACS-PRF#29083-AC7).

REFERENCES

1 Peterlin, A. *J. Macromol. Sci.* 1975, **B11**, 57
2 Kulkarni, M. G. and Mashelkar, R. A. *Polymer* 1981, **22**, 1655
3 Lasoski, S. W. and Cobbs, W. H. *J. Polym. Sci.* 1959, **36**, 21
4 Wunderlich, B. 'Macromolecular Physics, Volume 1: Crystal Structure, Morphology Defects', Academic Press, New York, 1973
5 Wunderlich, B. 'Macromolecular Physics, Volume 2: Crystal Nucleation, Growth, Annealing', Academic Press, New York, 1973
6 Ergoz, E., Fatou, J. G. and Mandelkern, L. *Macromolecules* 1972, **5**, 147
7 Lustiger, A. and Markham, R. L. *Polymer* 1983, **24**, 1647
8 Ludwig, B. W. and Urban, M. W. *Polymer* 1992, **33**, 3343
9 Ludwig, B. W. and Urban, M. W. unpublished work
10 Klein, J. *J. Polym. Sci., Polym. Phys. Edn* 1977, **15**, 2057
11 Peterlin, A. *Colloid Polym. Sci.* 1987, **265**, 357
12 Ludwig, B. W. and Urban, M. W. *Polymer* 1994, **35**, 5130
13 Ludwig, B. W. and Urban, M. W. *Polymer* 1993, **34**, 3377
14 Wunderlich, B. 'Macromolecular Physics', Vol. 2, Academic Press, New York, 1973
15 Nakagawa, K. and Ishida, Y. *J. Polym. Sci., Polym. Phys. Ed* 1973, **11**, 2153